

Single crystal elasticity of gold (Au) up to ~20 GPa: Bulk modulus anomaly below ~5 GPa and implication for a primary pressure scale

*Akira Yoneda¹, Hiroshi Fukui², Gomi Hitoshi¹, Seiji Kamada⁴, Longjian Xie¹, Naohisa Hirao⁵, Hiroshi Uchiyama⁵, Satoshi Tsutsui⁵, Alfred Baron³

1. Institute for Planetary Materials, Okayama University, 2. Graduate School of Material Science, University of Hyogo, 3. Materials Dynamics Laboratory, RIKEN SPring-8 Center, 4. Graduate School of Science, Tohoku University, 5. Japan Synchrotron Radiation Research Institute

We measured single crystal elasticity of gold (Au) as well as its lattice parameters simultaneously under high pressure by using inelastic X ray scattering (IXS) technique. Generated pressure and elastic moduli of gold were obtained only from the present experimental data at five pressure points between 0 and 20 GPa by direct numerical integration. Pressure variation of the bulk modulus displays an anomalous behavior; it is nearly constant up to ~5 GPa, and then steeply increases toward higher pressure. Similar anomaly is observed in independent first-principles calculations as well. The absolute pressure scale determined from the present results gives systematically lower pressures than those from the previous pressure scales owing to the bulk modulus anomaly founded in this study.

Keywords: gold, single crystal elasticity, bulk modulus, pressure scale, inelastic X ray scattering, diamond anvil cell

High-pressure phase transitions of MgCO₃ under the lower mantle conditions

*Fumiya Maeda¹, Seiji Kamada², Tatsuya Sakamaki¹, Naohisa Hirao³, Yasuo Ohishi³, Akio Suzuki¹

1. Department of Earth Sciences, Graduate School of Science, Tohoku University, 2. Frontier Research Institute for Interdisciplinary Sciences, Tohoku University, 3. Japan Synchrotron Radiation Research Institute

MgCO₃ is one of the important carbonate minerals in the deep Earth because it can be a carbon carrier from the surface to the mantle in subduction processes. Such deep carbonates may be involved in melting of subducted rocks and formation of deep diamonds in the mantle transition zone or lower mantle. MgCO₃ has especially been suggested to be the most stable carbonate under the high-pressure and temperature conditions.

Recent experimental and theoretical studies reported high-pressure phase transitions of MgCO₃ under the lower mantle conditions. A report of the high-pressure polymorph was started from 'magnesite II' at 115 GPa in Isshiki et al. (2004). Several recent studies supported a monoclinic MgCO₃ ('phase II') as a post-magnesite phase above ~80 GPa.

Phase II was revealed to be composed of (C₃O₉)-ring units which were constituted by three CO₄ tetrahedra sharing three oxygen atoms. However, the structure of phase II has a little difference between the previous studies: the space groups of phase II were reported as C2/m and P2₁/c in Oganov et al. (2008) and Boulard et al. (2011), respectively. Moreover the latest study by Pickard and Needs (2015) observed a new high-pressure polymorph having a triclinic lattice as a post-magnesite phase above 85 GPa, which changed to phase II at 101 GPa.

In addition to the difference of the post-magnesite phase and phase-II structures, none of the above studies decided the phase boundary of the high-pressure phase transitions at high temperature.

Therefore, we have been studied the phase relation of MgCO₃ up to the lowermost mantle conditions based on high-pressure and temperature experiments. We especially focused on the phase boundary of the high-pressure polymorphs at high temperature and a true post-magnesite phase.

The starting material was a natural magnesite from Bahia in Brazil. The experimental conditions were up to 138 GPa and 2900 K generated using a double-sided laser-heated diamond anvil cell (LHDAC). Culet diameters of diamond anvils used were between 130 and 250 μm. The sample was loaded into a sample chamber in a tungsten gasket which was pre-indented to 40–60 μm in thickness and drilled a 60–80-μm hole in diameter. Laser heating was conducted using a fiber laser. Pt or Au was used as a laser absorber. Run products were detected using synchrotron X-ray diffraction (XRD) measurements at beamline BL10XU of SPring-8 in Hyogo, Japan. Experimental pressures were measured using a thermal equation of state of Pt or Au (Fei et al., 2007) and thermal pressures were calculated using Mie-Grüneisen-Debye model (e.g., Fei et al., 1992). XRD patterns were analyzed using IPAnalyzer and PDIndexer software (Seto et al., 2010).

We observed the two high-pressure polymorphs of MgCO₃, which might be monoclinic phase II and triclinic phase reported in Oganov et al. (2008) and Pickard and Needs (2015), respectively. Phase II was observed mainly above 90 GPa and the lattice constants were estimated to be $a = 8.209 \text{ \AA}$, $b = 6.575 \text{ \AA}$, $c = 6.978 \text{ \AA}$, $\beta = 104.06^\circ$, and $V = 365.3 \text{ \AA}^3$ at $100 \pm 2 \text{ GPa}$ and $2080 \pm 230 \text{ K}$ when fitted using the Oganov's space group, C2/m. The triclinic phase might be appeared as a post-magnesite phase around 90 GPa: The XRD patterns were not explained only by magnesite and phase II. Strong peaks near 104 diffraction of magnesite are considered to be derived from the triclinic phase although we could not fit their patterns and estimate the lattice constants due to lack of the peak number to fit the triclinic unit cell. We could estimate the phase boundaries of high-pressure polymorphs based on the above observations.

The triclinic post-magnesite phase may have a very narrow stability field in the P-T phase diagram. The triclinic phase might buffer the significant structural change from magnesite (CO_4 triangles) to phase II (C_3 O_9 rings composed of three CO_4 tetrahedra).

Keywords: magnesite, high-pressure polymorph, lower mantle, LHDAC

What can mineral physics tell us about the origin of ULVZs?

*Catherine McCammon¹, Razvan Caracas²

1. Bayerisches Geoinstitut, University of Bayreuth, Germany, 2. Ecole Normale Supérieure de Lyon, France

The core-mantle boundary region is complex. In addition to large regions with reduced shear velocities (LLSVPs), there are small areas with shear velocities up to 30% lower than surrounding material, the so-called ultralow velocity zones (ULVZs). Although these heterogeneous regions are small (10 to 100 km), they have featured in speculation regarding an ancient global magma ocean, magnetic pole positions during reversals, core-mantle material exchange and the source of mantle plumes. Mineral physics provides important constraints in understanding the nature of ULVZs through the comparison of seismic data with experimental and computational studies of the relevant phases. Shear wave velocities are particularly important, and nuclear inelastic scattering (NIS) offers the attractive possibility to measure these velocities for iron-containing minerals in the laser-heated diamond anvil cell through direct measurement of the partial density of states (DOS). Complementary determination of the partial DOS using density functional theory (DFT) has shown the potential to identify experimental features that impact the velocity determination as demonstrated by our recent study on bridgmanite. We performed first-principles calculations to determine the iron partial DOS for $\text{Mg}_{0.75}\text{Fe}_{0.25}\text{SiO}_3$ post-perovskite. We calculated Debye sound velocities (which are closely related to the shear wave velocities) using the same approach as for experimental NIS data, and obtained velocities for $\text{Mg}_{0.75}\text{Fe}_{0.25}\text{SiO}_3$ post-perovskite that are consistent with literature values for MgSiO_3 and FeSiO_3 post-perovskite also calculated using DFT. In contrast, literature data on the Debye sound velocity determined experimentally using NIS is 35% lower than our calculated value, which led to previous suggestions that ULVZs originate from regions containing iron-rich post-perovskite. Our results show, however, that the lower NIS velocities in post-perovskite data likely arise from a similar artefact as the NIS bridgmanite data. The velocities derived from the DFT DOS of both bridgmanite and post-perovskite are consistent with seismic velocities of the bulk lower mantle, suggesting that ULVZs are likely not caused by iron-rich post-perovskite. Instead we favour previous suggestions that dense melts are a more plausible explanation.

Keywords: lower mantle, density functional theory, nuclear inelastic scattering, shear wave velocity, post-perovskite

Single crystal synthesis of δ -(Al,Fe)OOH using multi-anvil apparatus

*Itaru Ohira¹, Takaaki Kawazoe², Takayuki Ishii², Tiziana Boffa Ballaran², Catherine McCammon², Akio Suzuki¹, Eiji Ohtani^{1,3}

1. Department of Earth and Planetary Materials Science, Graduate School of Science, Tohoku University, 2. Bayerisches Geoinstitut, University of Bayreuth, 3. V.S. Sobolev Institute of Geology and Mineralogy, Siberian Branch, Russian Academy of Sciences

δ -AlOOH is an important hydrous mineral for understanding the water cycle in the deep Earth. In a descending slab, δ -AlOOH forms a solid solution with Phase H (MgSiO_4H_2) and ϵ -FeOOH [e.g., 1, 2]. This solid solution can transport water stored in its crystal structure to the deep mantle because it can be stable at the lowermost mantle conditions [1, 3]. Therefore, δ -AlOOH - Phase H - ϵ -FeOOH solid solution may affect the Earth's deep water cycles, chemical heterogeneity, and anomalies of seismic wave velocities at the lower mantle.

However, the stability, structure, elasticity, and spin state of this solid solution that are essential to discuss the issues above have not been constrained experimentally because of the difficulty to synthesize this solid solution as a homogeneous single phase.

In this study, we successfully synthesized Fe-bearing δ -AlOOH (δ -(Al, Fe)OOH) single crystals. Single crystals of pure δ -AlOOH and δ -(Al, Fe)OOH with dimensions up to ~ 0.6 mm were synthesized by a high-pressure hydrothermal method. Synthesis experiments were performed at 21 GPa and 1480 K for 4 h using a Kawai-type multi-anvil apparatus. Mössbauer spectra showed 95-100% $\text{Fe}^{3+}/\Sigma \text{Fe}$ at the octahedral site in δ -(Al, Fe)OOH. Unit-cell parameters of δ -AlOOH were consistent with those of previous studies, and they increased linearly with $\text{Fe}/(\text{Al}+\text{Fe})$ of the starting materials. The crystals contain 1-2 wt.% of excess water compared to their ideal water content. The syntheses of large single crystals of δ -(Al, Fe)OOH will facilitate investigations of their stability, elasticity, elastic anisotropy, spin state, and behavior of hydrogen bonding, which will improve our understanding of the water cycles, chemical heterogeneity, and anomalies of V_p and V_s in the deep Earth.

This work was supported by the JSPS Japanese-German Graduate Externship.

Reference

- [1] Ohira et al. (2014) *Earth and Planet. Sci. Lett.*, **401**, 12-17
- [2] Liu et al. (2016) *Goldschmidt Conference 2016*, **04d**, 10:45-11:00
- [3] Sano et al. (2008) *Geophys. Res. Lett.*, **35**, L03303

Keywords: Water Cycle in the Earth's Interior, High Pressure and High Temperature Experiment, δ -AlOOH, ϵ -FeOOH, Single Crystal, Kawai-type Multi-anvil Apparatus

Pressure-induced stacking disorder and non-symmetric hydrogen bond in boehmite

Yusuke Ishii¹, *Kazuki Komatsu¹, Satoshi Nakano², Shinichi Machida³, Takanori Hattori⁴, Asami Sano-Furukawa⁴, Hiroyuki Kagi¹

1. Geochemical Research Center, Graduate School of Science, The University of Tokyo, 2. National Institute for Materials Science, 3. Neutron Science and Technology Center, CROSS-Tokai, 4. J-PARC Center, JAEA

It has gradually been accepted that significant amount of 'water' can exist as hydrous minerals in the deep Earth, at least locally at subducting slab or mantle transition zone, from the observation of high-P and high-T experiments and diamond inclusions (e.g., Peacock (2000) *Science*, **248**, 329; Pearson *et al.* (2014) *Nature*, **507**, 221). Because the main rock-forming minerals in the deep Earth are oxide or silicate minerals, hydrogens in hydrous minerals are surrounded by oxygens, and they form O-H...O hydrogen bonds (H-bonds). At high pressure, H-bond symmetrization may occur owing to the shortening O...O distances, yielding the O-H and H...O distances are equivalent, so that H-bonds in hydrous minerals occurred under some depth could be symmetrized. However, there are only a few studies regarding the H-bond symmetrization in hydrous minerals (e.g., Tsuchiya *et al.* (2002) *Geophys Res Lett*, **29**, 1; Sano-Furukawa *et al.* (2009) *Am Mineral*, **94**, 1255; Tsuchiya and Mookherjee (2015) *Sci Rep*, **5**, 15534), and little is known about the relation between H-bond symmetrization with compression and the physical property change. Here we show a structure variation of boehmite with increasing pressure observed by using in-situ x-ray/neutron diffraction methods and Raman spectroscopy under pressure, and first found that pressure-induced stacking disorder would prevent H-bond symmetrization.

Keywords: Boehmite, High Pressure, Stacking disorder

Dehydration kinetics of boehmite and diaspore

*Takaya Nagai¹, Kankichi Hattori², Jun Kawano¹, Ayako Shinozaki¹

1. Department of Earth & Planetary Sciences, Faculty of Science, Hokkaido University, 2. Division of Earth & Planetary Sciences, School of Science, Hokkaido University

Boehmite and diaspore are polymorphs of AlOOH . Dehydration kinetics of boehmite (H-boehmite), deuterated boehmite (D-boehmite) and diaspore were investigated by thermogravimetric measurements with various heating rates. During dehydration treatments, boehmite and diaspore convert to $\gamma\text{-Al}_2\text{O}_3$ and corundum, respectively. The extent of dehydration as a function of temperature and heating rate was analyzed by integral isoconversional methods proposed in Vyazovkin et al.(2011). Because obtained isoconversional activation energies vary significantly with conversion extent, dehydration processes of these hydrous minerals are dominated by not a single reaction but multiple reaction steps. Comparison between H-boehmite and D-boehmite suggests the early stage of dehydration process is controlled by hydrogen migration from one O-H group to adjacent O-H (formation of adsorbed water molecule). On the other hand, comparison between H-boehmite and diaspore suggests the latter stage of dehydration process is controlled by migration of the adsorbed water molecule.

Keywords: dehydration kinetics, boehmite, diaspore

Molecular Dynamics Study of Soret Effect in Calcium-Aluminosilicate glass

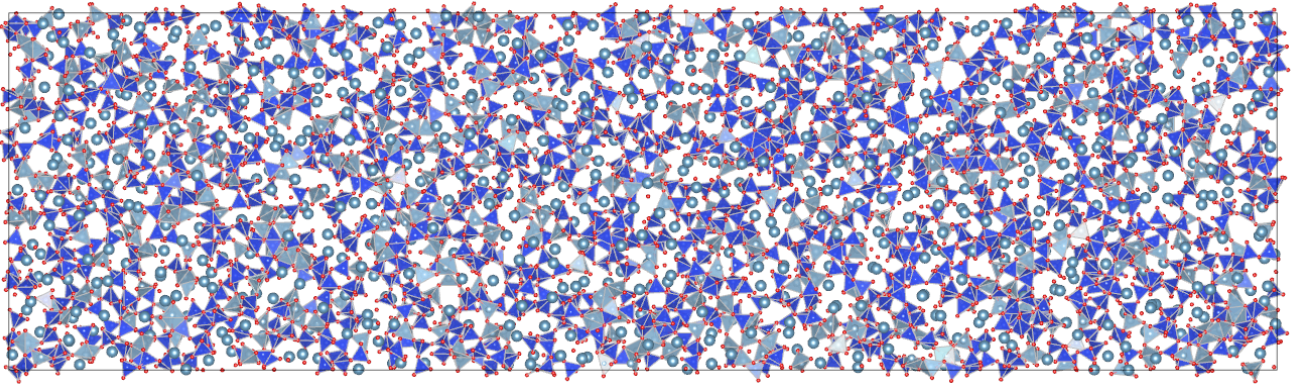
*Fumiya Noritake¹, Yukihiro Yoshida², Hirofumi Hidai³, Tetsuo Kishi², Nobuhiro Matsushita², Tetsuji Yano²

1. Graduate Faculty of interdisciplinary Research, University of Yamanashi, 2. Department of Materials Science and Engineering, Tokyo Institute of Technology, 3. Department of Mechanical Engineering, Chiba University

There are various transportation phenomena driven by a potential gradient. The Soret effect has been known as the diffusion driven by a temperature gradient (Soret, 1879; Ludwig, 1856). While the inverse one is known as Dufour effect. The Soret effect is sometime used in the explanation of fractionation phenomena in geology (Leshner, 1986; Dominguez et al., 2011). Recently Kishi et al. (2016, conference abstract) reports a distribution anomaly of composition around the trace of the migration of high-temperature metal sphere induced by laser irradiation in calcium aluminosilicate glass (Hidai et al., 2016). The rate of fractionation by temperature gradient is determined by both thermal diffusivity (D_T) and mass diffusivities (D) because the total net flux must be zero in a steady state. Consequently, understanding the Soret effect and determination of Soret coefficient (D_T/D) are difficult because the coefficient is affected by not only atomic mass and inter-atomic interaction that affect activation energy but also geometric/structural factor. Calcium-aluminosilicate system is suitable for the investigation of the Soret effect because three oxides have different characteristics; namely, network former, network modifier, and intermediate oxide.

We applied the molecular dynamics (MD) simulations for this system to investigate the mechanism of fractionation by temperature gradient. The MD simulation is an appropriate method for this study because it gives trajectories of each atoms in the simulation cells and potentials of each atom at any point in simulation time. MD simulations of $\text{Ca}_3\text{Al}_2\text{Si}_6\text{O}_{18}$ glass were performed using MXDORTO code (Sakuma & Kawamura, 2009). The simulation conditions are as follows: The inter-atomic potential model was taken from Noritake et al. (2015). System of approximately 30000 particles in rod-shaped (approximately $5 \times 5 \times 17$ nm) simulation cell in periodic boundary condition was firstly annealed for 2 ns at 1873 K from randomly generated structure. Then the liquid was quenched to room temperature at the rate of 10^{12} K/s. Then we started the simulations in temperature gradient. The temperatures in sliced regions (approximately 0.35 nm thickness) perpendicular to the longest axis at the end and the center of simulation cell were maintained 300 and 3500 K using the scaling procedure, respectively. After several tens nano-second simulations, we confirmed the changes in distribution of composition. The concentration of SiO_2 in the high-temperature center part slightly increases as simulation proceeds. In contrast the concentration of CaO in that part slightly decreases. The distribution of concentration of Al_2O_3 does not change apparently. Quantification of coefficient and mechanisms will be discussed in this presentation.

Keywords: Molecular Dynamics, Silicate Glass, Silicate Melt, Soret Effect



Phase transition of AlPO_4 -moganite: In-situ high-temperature Raman spectroscopic study

*Masami Kanzaki¹

1. Institute for Planetary Materials, Okayama University

Moganite-form of AlPO_4 has recently discovered as one of high-pressure phases (Kanzaki and Xue, 2012). Moganite is one of rare polymorphs of SiO_2 , and its structure is closely related to twinned quartz. For SiO_2 -moganite, temperature-induced displacive transition has been reported (Heaney et al., 2007). However, pure phase sample is difficult to obtain, and accordingly quality of data by Raman or diffraction is not good. Although AlPO_4 -moganite is easy to get pure phase, it is metastable at ambient pressure (moganite- SiO_2 is not stable phase either). In this study, phase transition in AlPO_4 -moganite was explored using in-situ high-temperature Raman spectroscopy up to 800 °C at ambient pressure. This transition was briefly mentioned in our 2011 this session talk, but completely new dataset, and additional low frequency data were obtained, and will be presented.

Used sample was same as that reported in our previous study (Kanzaki and Xue, 2012), and was synthesized at 5 GPa and 1500 °C. For heating, a wire heater was used (Kanzaki et al., 2012).

Temperature was calibrated using 5~6 substances with known melting points. For Raman measurement, a home-built confocal micro-Raman system was used (488 nm laser, ~80 mW, 500 mm polychromator, liquid N_2 cooled CCD detector). Initially, frequency region higher than 100 cm^{-1} was observed to 800 °C. Recently, our system is able to measure low frequency region, and two new peaks were identified at about 60 and 73 cm^{-1} at room temperature (see my talk last year). In order to check these peaks are soft mode or not, additional high-temperature study was conducted for < 100 cm^{-1} region. For the measurement, anti-Stokes and Stokes regions were observed simultaneously to identify true Raman peaks from the peaks originated from instrumental artifacts. The temperature is increased by 25 °C step, and increased up to 800 °C.

For the spectra measured above 100 cm^{-1} , several hard Raman modes displayed small shift to lower frequency with temperature. Above 425 °C, this trend was reversed or became nearly constant, and no discontinuity was observed. These results suggest that there is a displacive (higher order) phase transition at about 425 °C. For the region below 100 cm^{-1} , the 73 cm^{-1} peak showed significant temperature shift to lower frequency accompanied with significant broadening on the peak width. The peak disappeared at 475 °C. From these results, this peak is considered as soft mode. The 60 cm^{-1} peak shifted just like the hard mode noted above, and still remained above 475 °C. At around 800 °C, berlinite (stable phase) was observed.

Our study confirmed that AlPO_4 -moganite indeed has the displacive transition, and identified soft mode. For SiO_2 -moganite, only hard mode Raman was observed, and the transition temperature was determined as ~ 570 K (Heaney et al., 2007). No soft mode was reported to date. Our study suggests that soft mode for SiO_2 -moganite may exist at lower frequency region not studied yet. There is some differences in the transition temperature between obtained from hard mode and from soft mode. This is likely due to thermal non-equilibrium in the sample as heating rate was faster for latter (low frequency run). Further study including remeasurement and measurement at cooling process is in progress.

Heaney, P.J. et al. (2007) *Am. Mineral.*, 92, 631

Kanzaki, M. and Xue, X. (2012) *Inorg. Chem.*, 51, 6164

Kanzaki, M. et al. (2012) *J. Min. Petrol. Sci.*, 107, 114

Keywords: AlPO₄-moganite, soft mode, Raman spectroscopy

Symmetry reduction of analcime with Al/Si ordering

Neo Sugano¹, *Atsushi Kyono¹

1. Graduate School of Life and Environmental Sciences, University of Tsukuba

Analcime is a sodium aluminosilicate hydrate ($\text{NaAlSi}_2\text{O}_6 \cdot \text{H}_2\text{O}$) with the ANA type of zeolite framework. It occurs widely in hydrothermal and diagenetic environments. Symmetry of analcime is well known to be changed with distribution of framework cations and extra-framework cations. Naturally occurring analcime generally exhibits cubic symmetry space group $la-3d$, which is the maximum topological symmetry, but it can crystallize in at least three different symmetries; tetragonal space group $I4_1/acd$, orthorhombic space group $lbca$, and monoclinic space group $I2/a$. However, crystallization conditions affecting the symmetry change have not been fully understood yet. In the study, we hydrothermally synthesized single crystals of analcime and hydrothermally re-heated under various heating time. Single crystals obtained from the different processes were refined by using single-crystal X-ray diffraction method.

Single crystals ranging in size from 50 to 120 μm were grown from gels of $\text{Al}_2(\text{SO}_4)_3$ and Na_2SiO_3 . They show deltoidal icositetrahedron habit with well-developed 24 equivalent $\{2\ 1\ 1\}$ crystal faces. Single crystals grown from gels possess cubic $la-3d$ symmetry, in which Si and Al are totally disordered over the framework T sites. Single crystals of analcime hydrothermally reheated for 24h, however, exhibit tetragonal $I4_1/acd$ symmetry. The tetragonal analcime shows a weak site preference of Si for $T1$ site and Al for $T2$ site. Single crystals of analcime hydrothermally reheated for 48h display orthorhombic $lbca$ symmetry. In the orthorhombic analcime, Si and Al are strongly ordered over the T sites. Si is preferentially distributed into $T11$ and $T12$ sites whereas Al is into $T2$ site. The crystal structural analysis revealed continuous symmetry reduction from cubic $la-3d$ to orthorhombic $lbca$ through tetragonal $I4_1/acd$ depending on heating time. On the other hand, Na atoms are equally distributed over the extra-framework sites during the symmetry reduction. The result of the study clearly shows the heating time significantly influences the Al/Si ordering over the framework T sites rather than the ordering of extra-framework cations. The symmetry reduction in analcime would be useful for understanding of petrological and geochemical history of rocks.

Keywords: analcime, single-crystal X-ray diffraction, Al/Si ordered distribution

Reexamination of the crystal structure of artinite, $\text{Mg}_2\text{CO}_3(\text{OH})_2 \cdot 3\text{H}_2\text{O}$, with two-dimensional disorder

*Gen-ichiro Yamamoto¹, Atsushi Kyono¹

1. Life and Environmental Sciences, University of Tsukuba

Artinite is a magnesium carbonate hydrate mineral with the formula $\text{Mg}_2\text{CO}_3(\text{OH})_2 \cdot 3\text{H}_2\text{O}$. It is known to possess a disordered structure in which carbonate groups and water molecules alternate statistically along *b*-axis (Akao and Iwai 1977). The Mg atoms are octahedrally coordinated by three hydroxyl groups, two water molecules, and one O(1) atom, and arranged in infinite chains parallel to *b*-axis by sharing edges. In the structure, half of the O(1) atoms is bounded to carbonate groups and the other half is to water molecules. It is therefore possible that in the disordered structure a carbonate group is arrayed at the next of a carbonate group along *b*-axis. However, if a carbonate group is positioned at the next of a carbonate group, the O-O distance between the carbonate groups is 0.894 Å, which is apparently shorter than the van der Waals radius of an O atom (1.40 Å). On the other hand, if the carbonate groups and water molecules strictly alternate along *b*-axis, a periodicity of two unit cell should appear along the *b*-axis. In the study, we reexamined the crystal structure of artinite and reconsidered the disordered configuration of carbonate group and water molecule in the structure.

Naturally occurring artinite (San Benito, USA) was used in the study. Single-crystal X-ray diffraction measurements were performed using Bruker APEXII ULTRA single-crystal diffractometer equipped with a CCD detector, multilayer optics, and graphite monochromated $\text{MoK}\alpha$ radiation ($\lambda = 0.71073$ Å) generated by a rotating anode. X-ray data were collected at a temperature of -173 °C using a N_2 -gas-flow cryostat. The crystal structure was solved by intrinsic phasing in the APEX2 software package and refined by full-matrix least squares using Shelxl-97 (Sheldrick, 1997). Computational chemistry calculations were performed using Gaussian 09 program (Frisch et al., 2009). Mulliken charges were calculated using Density Functional Theory (DFT) at B3LYP employing 6-31G basis set.

The refined cell parameters are $a = 16.468(8)$ Å, $b = 3.1352(15)$ Å, $c = 6.184(5)$ Å, $\beta = 98.702(5)$ °, space group $C2/m$. The unit cell corresponds to the totally disordered configuration of carbonate groups and water molecules on the *b*-lattice. The structure refinement converged to $R1 = 0.0339$, $wR2 = 0.0937$, and $Goof = 1.013$ for 414 reflections with $F_o > 4s(F_o)$. The bond distances in the MgO_6 octahedron are 2.0345(9) Å (×2), 2.0610(13) Å, 2.1641(9) Å (×2), and 2.0135(13) Å. Those in the carbonate group are 1.227(3) Å and 1.2920(18) Å (×2). When the carbonate group is located at the next to the carbonate group along *b*-axis, the O-O distance between the neighboring O atoms in the carbonate groups is 0.8816(19) Å. The Mulliken charges of the neighboring O atom, O atom on the opposite side, and O atom bounded to Mg atom are -0.378, -0.721, and -0.845, respectively. That of C atom is 1.296.

Crystal structures of magnesium carbonate (hydrate) minerals are always composed of MgO_6 octahedra. Compared with the MgO_6 octahedra constituting hydromagnesite $\text{Mg}_5(\text{CO}_3)_4(\text{OH})_2 \cdot 4\text{H}_2\text{O}$, nesquehonite $\text{MgCO}_3 \cdot 3\text{H}_2\text{O}$, and magnesite MgCO_3 , the MgO_6 octahedron in artinite displays a large quadratic elongation parameter (Robinson et al. 1971). In addition, the carbonate group in artinite can be characterized by highly distorted geometry forming an acute isosceles triangle. The results of crystal structural analysis are in good agreement with those of previous research (Akao and Iwai, 1977). Furthermore, our study completely supports the conclusion obtained in the early study that every chain running along *b*-axis has two possible positions of carbonate groups and water molecules, thus producing the two-dimensional disorder. The reason why the carbonate groups can be located at an unusual short distance would be explained by the strongly polarized charge distribution within the carbonate groups.

Keywords: Artinite, disordered configuration, single crystal structure analysis, ab initio calculation

Experimental investigation of the Fe₂O₃-As₂O₅ system in air

*Pierre Hudon¹, In-Ho Jung

1. McGill Univ.

Arsenic is notoriously harmful to the environment. In numerous deposits and mining concentrates, it is usually present in the form of sulfides such as arsenopyrite (FeAsS) and enargite (Cu₃AsS₄), arsenides such as loellingite (FeAs₂) and nickeline (NiAs), arsenates such as scorodite (FeAsO₄·2H₂O), annabergite (Ni₃(AsO₄)₂·8H₂O) and erythrite (Co₃(AsO₄)₂·8H₂O) and solid solution in ore minerals such as chalcopyrite (CuFeS₂), pyrite (FeS₂), and sphalerite (Zn, Fe)S, for example. Currently, scorodite is the mineral of choice to immobilize arsenic from mine wastes because it has a very low solubility in water. Scorodite is also the most common arsenate known in nature where it is found in hydrothermal deposits and as a secondary mineral in gossans. Unfortunately, there is a lack of information in the literature regarding arsenate systems, which hamper the understanding of the complex chemical reactions involved in their genesis. In the last decades, much effort has thus been devoted to determine the thermodynamic properties and phase relations of arsenates in hydrous and anhydrous conditions. In this regard, the Fe₂O₃-As₂O₅ system is of particular interest because it contains the compound FeAsO₄, the anhydrous analog of scorodite. Surprisingly though, the system Fe₂O₃-As₂O₅ is still poorly known. This is due to the hygroscopic nature, slow kinetics, and high volatility of its phases, and to the presence of iron, which prevent the use of platinum crucibles at high temperature. The first (and only) experimental investigation of the whole phase diagram was performed by Kasenov and Mustafin [*Russ. J. Inorg. Chem. (Engl. Transl.)*, 1997, 42, 1598-1599] using differential thermal analysis (DTA) and X-ray diffraction (XRD) up to 1100 °C. Unfortunately, experiments were performed in sealed but evacuated (to 10⁻⁶ bar, i.e. 10⁻³ mm Hg) silica crucibles and as a result, evaporation probably occurred during the runs. Moreover, the silica crucibles may have reacted with the starting materials, modifying the melting point of the solid phases and the oxidation state of both As and Fe in the system. Consequently, the experimental data collected by Kasenov and Mustafin (1997) may have produced a very different phase diagram than the one expected in air. To determine the correct Fe₂O₃-As₂O₅ phase diagram in air and minimize most of the problems cited above (hygroscopicity, slow kinetics, high volatility, and presence of Fe reacting with crucibles), we prepared dry starting materials, carried out long duration experiments (up to 36 days) with non-evacuated sealed Au₇₅Pd₂₅ crucibles up to 1000 °C using the quenching method and accomplished phase characterization using XRD, backscattered electron (BSE) imaging, and electron probe microanalysis (EPMA). Based on our experiments, new subsolidus phase relations are proposed for the Fe₂O₃-As₂O₅ phase diagram in air, which are significantly different from the ones published earlier by Kasenov and Mustafin (1997). We also report the existence of a new compound, Fe₆As₄O₁₉ (F₃A₂), which is a potential candidate for arsenic sequestration.

Keywords: Phase diagram, Iron arsenates, Scorodite, Fe₆As₄O₁₉

Quantitative determination of Al/Si-order parameter in sillimanite from micrometric region using HARECX method

*Yohei Igami¹, Takahiro Kuribayashi², Akira Miyake¹

1. Graduate School of Science, Kyoto University, 2. Graduate School of Science, Tohoku University

Sillimanite is one of the polymorphs of Al_2SiO_5 which are valuable as indicators of pressure and temperature. Structure of sillimanite consists of AlO_6 octahedral chains and Si/AlO_4 tetrahedral double chains parallel to the *c*-axis. Although the tetrahedral Si/Al ions are normally ordered, a possibility of its disordering at high temperatures has been suggested (e.g. Zen, 1969). However, the Al/Si-order parameter of sillimanite has not been successfully quantified. The main problems are that one is the difficulty of separating mullite ($\text{Al}_2[\text{Al}_{2+2x}\text{Si}_{2-2x}]\text{O}_{10-x}$, $x \cong 0.17-0.59$) from sillimanite, because mullite is very similar to sillimanite crystallographically, and another is the difficulty to distinguish Al from Si using XRD experiments because of similarity of their X-ray scattering factor.

On the other hand, Atom location by channeling-enhanced microanalysis (ALCHEMI) using TEM-EDS was carried out for determination of Al/Si-order parameter in orthoclase by Taftø & Buseck (1983). By ALCHEMI, it can distinguish the elements with similar atomic number, e.g. Al and Si, and it can be quantified the Al/Si-order parameter from the only sillimanite micrometric region. Furthermore, HARECX (High Angular Resolution Electron Channeling X-ray Spectroscopy), which was developed from ALCHEMI recently (e.g. Soeda, 2000; Yasuda *et al.*, 2006), provides more quantitative information, because of many EDS measurements by varying the direction of incident electron beam. In this study, therefore, HARECX experiments were carried out on sillimanite to establish the determination procedure for the Al/Si-order parameter in sillimanite.

Sillimanite crystals in Rundvågshetta, East Antarctica, which are homogeneous without characteristic textures, were examined using TEM-EDS (JEOL JEM-2100F, JED-2300T). HARECX profiles were obtained by collecting X-ray signals as a function of electron-beam direction. The Al/Si-order parameter was determined by comparison between the obtained HARECX profiles and simulated HARECX profiles by program ICSC (Oxley & Allen, 2003). Additionally, CBED (convergent-beam electron diffraction) patterns were also obtained to estimate sample thickness. Moreover, single crystal X-ray diffraction experiment using an automated four-circle X-ray diffractometer (Rigaku, AFC-7S, Tohoku Univ.) with $\text{MoK}\alpha$ Radiation ($\lambda = 0.71069 \text{ \AA}$) was also carried out in order to evaluate the result obtained by HARECX.

As the result, the HARECX profiles were successfully obtained from $1.5 \mu\text{m}$ diameter region. For quantitative analysis, two types of profiles were simulated; a profile of ordered sillimanite and that of disordered sillimanite, using the sample thickness determined by CBED. The experimental profiles were successfully fitted to linear combination of the two simulated profiles, and Al/Si-order parameter was determined. The determined results of 18 measurements were converged around 0.80 regardless of sample thickness. However, single crystal XRD experiment showed the Al/Si-O bond distances corresponding to the Al/Si-order parameter of 0.88. The discrepancy are thought to be caused by estimation error of absorption coefficient of incident electron for sillimanite which is one of the simulation parameter to affect the HARECX simulation. It suggests that the additional absorption should be required for more precise simulation.

The above analytical procedure was also successfully applied to experimentally heat-treated sillimanite, avoiding mullite or glasses formed by heat-treatment. Furthermore, the HARECX method can also apply to various other minerals to determine site occupancies and estimate formation environment.

Keywords: ALCHEMI, HARECXS, sillimanite, order parameter, TEM

Melting relations in the system of MgSiO_3 – SiO_2 at high pressures

*Takuya Moriguti¹, Akira Yoneda¹, Eiji Ito¹

1. Institute for Planetary Materials, Okayama University

Melting relations in the MgO – SiO_2 system at high pressures have been extensively studied to simulate chemical differentiation in a deep magma ocean formed in the early stage of the Earth (e.g. Kato and Kumazawa, 1985; Ito and Katsura, 1992). Almost all of these works have been carried out on the compositions ranging from MgO to MgSiO_3 , assuming that the bulk mantle composition is peridotitic or close to that derived from CI chondrite. Recently enstatite chondrite (E-chondrite) was proposed as the bulk earth source material (Javoy et al., 2010) because the isotope systematics over O, N, Mo, Re, Os, and Cr for the Earth and Moon are almost identical to that of E-chondrite. In E-chondrite, the silicate composition is characterized by $\text{MgO}/\text{SiO}_2 = 0.5$ (in weight ratio) which is substantially lower than that of the peridotitic mantle (~ 0.85).

In this context, melting relations on compositions more SiO_2 enriched than MgSiO_3 are indispensable to clarify the mantle fraction. However, available information regarding phase relations in the system MgSiO_3 – SiO_2 is so far limited to 1 GPa. In the present study, therefore, we would determine the melting relations at pressures 5 to 20 GPa, focusing on the compositions of MgO - $x\text{SiO}_2$ ($x = 0.8$ to 1.2). We expect to present some new results.

Keywords: enstatite chondrite, melting relation, magma ocean, mantle differentiation, high pressure

Experimental study on the stability and physicochemical behavior of methane hydrate under high pressure and high temperature

*Hirokazu Kadobayashi¹, Hiroaki Ohfuji¹, Hisako Hirai², Ohtake Michika³, Yoshitaka Yamamoto³

1. Geodynamics Research Center, Ehime University, 2. Department of Environment Systems, Faculty of Geo-environmental Science, Rissho University, 3. National Institute of Advanced Industrial Science and Technology

Methane hydrate are thought to be an important constituent of icy bodies and their satellites, such as Neptune, Uranus and Titan. It is a clathrate compound composed of hydrogen-bonded water cages (host) and molecules or atoms (guests) included in the cages. Methane hydrate has an sI cage structure at low (< 0.8 GPa) pressures and room temperature. It transforms to an sH cage structure at approximately 0.8 GPa, which further transforms to a filled-ice Ih structure at approximately 1.8 GPa. The Ih structure consists of an ice framework similar to ice Ih and voids that are filled with methane molecules (e.g. Loveday et al. 2001; Shimizu et al. 2002). This structure was found to be stable up to at least 86 GPa, supporting that methane hydrate may be stable in the deep interior of icy bodies. Although the sequence of the phase transitions with pressure have been studied well at room temperature, there are only a few studies that addressed the stability of methane hydrate under high pressure and high temperature (Kurnosov et al., 2006; Bezacier et al., 2014). In addition, the pressure range of these previous studies is only limited to < 5 GPa. Therefore, a further investigation is needed to understand the stability and physicochemical behavior of methane hydrate under extreme conditions corresponding to the interior of icy bodies.

In this study, we carefully investigated the stability and decomposition mechanism of methane hydrate in an externally-heated diamond anvil cell in the range of 2-51 GPa and 298-653 K using in-situ Raman spectroscopy and X-ray diffraction. The results show that methane hydrate decomposes to ice VII and solid methane at temperatures considerably lower than the melting curves of solid methane and ice VII in the pressure range of 2-51 GPa. The decomposition conditions of methane hydrate that were obtained at high pressure may help in the modeling of the accretion process and evolutions of icy bodies.

Keywords: methane hydrate, high pressure and high temperature, gas hydrate, diamond anvil cell

Spin transition and thermal conductivity anisotropy of siderite under high pressure

*Keng-Hsien Chao^{1,2}, Wen-Cheng Owen Huang¹, Wen-Pin Hsieh²

1. National Central University, Taiwan, 2. Academia Sinica, Taiwan

Deep carbon cycle plays an important role in controlling the distribution of carbon between Earth's surface and interior. The subduction slabs transport the carbonates on seafloor into Earth's interior. Most of the carbons could be trapped in Earth's interior, and carbons recycled to the ground surface are rare. According to recent studies, Fe-bearing carbonates, for instance siderite, have been considered to be potential carbon hosting minerals inside the Earth's interior. Previous studies showed that the distribution of Fe-bearing carbonates in mantle is difficult to be detected by seismic observation due to their low concentration, yet there is strong elastic anisotropy in Fe-bearing carbonate which could be a potential diagnostic feature. In addition to their intrinsic elastic anisotropy, spin transition of Fe driven by extremely high pressure is another factor that could change the physical properties of siderite. For instance, the volume of siderite collapses sharply across spin transition and bulk modulus changes. However, thermal conductivity, which could control the thermal structure in Earth's interior and is related to the elastic properties of Fe-bearing carbonates, remains rarely studied. In this work, we study the vibrational spectrum and thermal conductivity of siderite along a-axis and c-axis from ambient condition to 65GPa under room temperature by Raman spectroscopy and Time-domain thermoreflectance combined with diamond anvil cell techniques. We found that the range of spin transition is 46GPa~52GPa, which is similar to previous studies, suggesting that iron concentration in siderite has minor effect on the pressure range of spin transition. Preliminary results show that the thermal conductivity of siderite along a-axis decreases across spin transition.

Keywords: siderite, spin transition, thermal conductivity

Crystal structure of protoenstatite quenched to ambient temperature

*Masami Kanzaki¹

1. Institute for Planetary Materials, Okayama University

Protoenstatite (MgSiO_3) is generally thought that it cannot be quenched to ambient temperature, however, there are several reports on quenched protoenstatite (e.g., Lee and Heuer, 1987). We also observed protoenstatite using ^{29}Si MAS NMR spectroscopy of MgSiO_3 sample taken out from a furnace and cooled down (Xue et al., 2002). However, there is no study on crystal structure of quenched protoenstatite nor quantitative analysis on proportion of enstatite polymorphs in the quenched samples. In this study, four samples with different cooling rates were studied by powder X-ray diffraction and micro-Raman spectroscopy.

Starting enstatite sample was prepared from reagent-grade MgO and SiO_2 , and they were mixed, and pelletized, and treated at 1500°C twice. In previous reports (Lee and Heuer, 1987; Reynard et al., 2008), glass or melt was quenched to obtain protoenstatite, but in the present study, ordinary solid state synthesis method was employed. The starting material was kept at 1500°C for 5h, and cooled down to ambient temperature with four different cooling rates (150 K/h, 15H/h, taken out from the furnace and bottom of Pt crucible was dipped into water, sample directly dipped into water). It is known that protoenstatite would transform to low-clinoenstatite by grinding. So the samples were handled gently. Since recovered samples were powder, no special treatment was necessary to put into sample holder for powder X-ray diffraction measurement. Grain size of all samples are similar, and are about 5 micrometer with angular shapes. The Rietveld method was used to refine crystal structure of protoenstatite, and quantitative analysis of the samples (RIETAN-FP program used). For Raman spectroscopic measurement, recipe proposed by Reynard et al. (2008) is used to identify enstatite polymorphs.

From X-ray diffraction, it was found that all samples contain both protoenstatite and low-clinoenstatite. Their existence was also confirmed by micro-Raman spectroscopy including the starting material. Structural refinement was conducted using protoenstatite-rich sample. Obtained lattice parameters are consistent with extrapolated values of high-temperature data (Jiang et al., 2002), suggesting no major structural change with temperature. Refined crystal structure of protoenstatite is essentially same as that determined at high temperature, and is consistent with simulated structure using the DFT calculation (at 0 K). Quantitative analysis by the Rietveld method revealed that about 40% protoenstatite exists in Pt crucible bottom dipped into water sample, and about 30% for slowly cooled sample (15 K/h), and there is cooling rate dependence for the proportion. However, supposedly most rapidly quenched sample, directly dipped into water, showed lowest proportion (30%).

Present study revealed that even using common synthesis technique, significant amount of protoenstatite is remained in so-called low-clinoenstatite sample. This implies that previous phase equilibrium studies of the MgSiO_3 system might used such samples, and reassessment of those studies may be necessary. As a such example, a possibility of incorrect phase relation between low-clinoenstatite and orthoenstatite due to overlooked protoenstatite will be discussed.

Jiang, D. et al. (2002) *J. Min. Petrol. Sci.*, 97, 20

Lee, W.E. and Heuer, A.H. (1987) *J. Am. Ceram. Soc.*, 70, 349

Reynard, B. et al. (2008) *J. Euro. Ceram. Soc.*, 28, 2459

Xue, X. et al. (2002) *Geochim. Cosmochim. Acta*, 66, A853

Keywords: crystal structure of protoenstatite, quantitative analysis by Rietveld method, enstatite phase relation

Measurements of fusion enthalpy of anorthite and diopside by combining techniques of drop calorimetry and solution calorimetry

*Toru Sugawara¹, Toshiaki Ohirra¹

1. Graduate School of Engineering Science, Akita University

Enthalpy of fusion of rock-forming minerals is required to calculate enthalpy of multicomponent silicate liquid and are of considerable importance in thermodynamic consideration and phase equilibrium calculation in igneous process. Fusion enthalpy of diopside has been measured by various methods. In contrast, few study has been reported an enthalpy of fusion of anorthite. We developed a twin conduction calorimeter and determined enthalpies of fusion of diopside and anorthite by combining drop calorimetry for molten diopside and anorthite and solution calorimetry for glasses.

First, differences of enthalpy of diopside and anorthite liquids between 1873-1773K and 273K were measured by drop calorimetry. Enthalpies of solution of the drop quenched glasses, anorthite glass annealed at 1100K for 72h and synthetic crystals of diopside and anorthite were determined by a hydrofluoric acid solution calorimetry. Measuring system of twin conduction calorimeter consists of sample and reference Teflon vessels placed on copper block and is immersed in a water thermostat. Approximately 50mg sample powders were reacted with 23wt% hydrofluoric acid solution, and then temperature difference of solution between both vessels was measured by thermistors. Enthalpy was calibrated by heating a resistance element.

Enthalpy of vitrification determined from difference of enthalpies of solution for quenched glass and crystal are 87.3 ± 7.0 kJ/mol for diopside and 83.4 ± 6.5 kJ/mol for anorthite. Enthalpy of fusion at melting point was calculated from the enthalpy of vitrification, relative enthalpy measured by drop calorimetry and published heat capacity of minerals. The enthalpy of fusion determined for diopside is 138.7 ± 7.0 kJ/mol at 1665K and is consistent with values reported in previous four studies (137-139 kJ/mol). The enthalpy of fusion of anorthite at melting point (1830K) is 145.0 ± 6.5 kJ/mol and 146.1 ± 7.5 kJ/mol when enthalpies of solution for quenched and annealed glasses are used, respectively. This is 10% higher than a value reported by Richet et al. (1984) (137.0 ± 7.0 kJ/mol). This discrepancy is probably caused by error in fictive temperature of glass sample used in solution calorimetry estimated in previous study.

Keywords: Silicate melt, Enthapy of fusion, Enthalpy of solution, Calorimetry

In situ hot/cool-stage AFM study on crystal growth of barite at 10 - 40°C

Wen Liu², *Yoshihiro Kuwahara¹, Keisuke Ootsuka², Masato Makio²

1. Faculty of Social and Cultural Studies, Kyushu University, 2. Graduate School of Integrated Sciences for Global Society, Kyushu University

Most global-scale geochemical phenomena begin with atomic-scale growth and dissolution reactions at the mineral-water interface. In situ Atomic Force Microscopy (AFM) allows direct observation of the growth and dissolution processes at the mineral-water interface at the site or step level. Many in situ and ex situ AFM studies on the dissolution reactions of the barite (001) surface have been conducted to elucidate the processes involved and problems mentioned above. However, to our knowledge, no in situ AFM study on mineral growth at low temperatures (below room temperature) has been reported. The dearth of low-temperature studies most likely owes to difficulties in constructing the AFM experimental system. Here we report the results of a experiment performed by in situ hot/cool-stage AFM observations of the growth behavior on the (001) surface of barite in supersaturated BaSO₄ solutions at 10 - 40°C. The mechanism of crystal growth of barite was characterized by the spiral growth mechanism where rhombic growth spirals elongated along the [010] direction were formed and the two-dimensional (2D) nucleation mechanism in which circular sector-shaped two-dimensional (2D) nuclei were formed and developed. In addition, the adhesive growth mechanism was observed only at 10°C.

The kinetic laws of the crystal growth on the barite (001) surface differed among crystallographic directions and crystal growth mechanisms. The advance rates of the two steps of 2D nuclei were proportional to the S . In contrast, the advance rates of the parallel steps with extremely short step spacing on growth spirals were proportional to S^2 , indicating that the lateral growth rates of growth spirals were directly proportional to the step separations. This dependence of the advance rate of every step on the growth spirals on the step separations predicts that the growth rates along the [001] direction of the growth spirals were proportional to S for higher supersaturations. The nucleation and growth rates of the 2D nuclei increased sharply for higher supersaturations using exponential functions. Only at 10°C, these rates changed to be proportional to S for higher supersaturations, indicating a change in main crystal growth mechanism from the 2D nucleation to the adhesive growth one. Two critical supersaturation points corresponding to the changes in main crystal growth mechanisms from the spiral growth, via 2D nucleation, to adhesive growth tended to decrease with decreasing of solution temperature.

Keywords: Barite, Crystal Growth, AFM

Characteristic local structures of Ca, Ti, Fe were observed in fusion glass of shergottite

*Tsubasa Tobase^{1,2}, Akira Yoshiasa¹, Massimo Nespolo², Hidetomo Hongu¹, Hiroshi Isobe¹, Maki Okube³, Hiroshi Arima³, Kazumasa Sugiyama³

1. Graduate School of Science, Kumamoto University, 2. Université de Lorraine, CRM2, UMR 7036, 3. Institute of Materials Research, Tohoku University

Shergottite is a kind of martian meteorite. Shergottite has the special glass structures which were melted at entering the Earth's atmosphere. The special metamorphism was observed in the local structures of melting glass which were affected by high temperature and rapid cooling at entering the Earth's atmosphere (Tobase et al., 2016). In order to obtain the information about coordination number, atomic distance and valence state at each ions, we performed local structural analysis of Ca, Ti, and Fe in shergottite by XAFS method. The estimation of environment at entering the Earth's atmosphere and getting out of the Mars were performed by local atomic structural analysis. In this study, the formation environment of melting glass is analyzed by comparison of local structures between those in shergottite and natural impact-related glass.

On the basis of the shape of XANES spectra in shergottite, local structures of Ca in shergottite are almost similar to those in tektite and meteorite fusion glass, although slight difference in XANES spectra is observed. This slight difference might come from the chemical composition and coordination environment. The similarities in XANES spectra between shergottite and the other fusion glasses indicate that formation environment of fusion glass in shergottite is almost similar to that in the other meteorite. Okudera et al., (2012); Wang et al., (2013) reported that the main peak position in Fe XANES spectra is related to valence state such as oxidation state of Fe ions, which was influenced by the surrounding oxygen during formation process. The main peak position of Fe XANES spectra in shergottite is similar to those in the other fusion glasses, thus fusion glass in shergottite was estimated to be formed under the Earth's atmosphere like the other fusion glasses. On the other hand, local structural information of Ti in shergottite is different trend to that in Ca and Fe. Since the Ti XANES spectra in shergottite is similar to those in darwin glass whose formation condition is different from the other impact-related glasses and fusion glasses, fusion glass in shergottite might be experienced unique formation process. Shergottite which originated from the Mars contains the fusion glass produced during entering the Earth's atmosphere and glass part influenced during getting out of the Mars. The local structure in fusion glass of unique and different from the other fusion glasses.

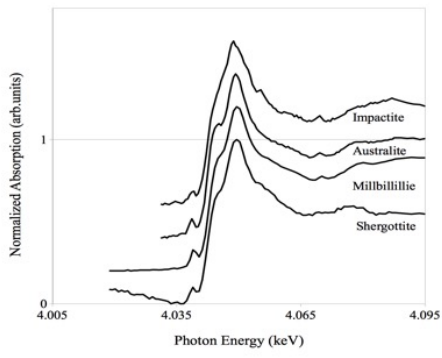
Reference

Tobase et al., (2016), IOP Conference series, 712, 012095.

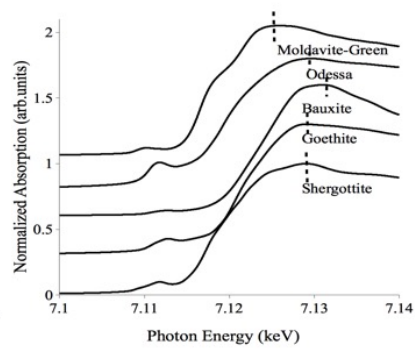
Wang et al., (2013), J. Miner. Petro. Sci., 108, 288-294.

Okudera et al., (2012), J. Miner. Petro. Sci., 107, 127-132.

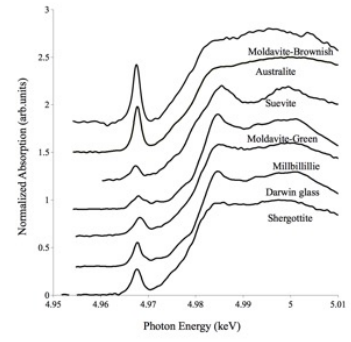
Keywords: Shergottite, Local structure of Ca, Ti, Fe, XANES, EXAFS, Fusion glass



(a) Ca XANES spectra



(b) Fe XANES spectra



(c) Ti XANES spectra

Anomalous characteristics of relative formation and reaction for terrestrial mineral crystals

*Yasunori Miura¹

1. Visiting (Yamaguchi, Foreign University (AIC University))

Mineral crystals are stored as databases in a global description with the physicochemical and earth science unit of rocks. However, description by identification of the minerals is based on the present environment through many solidified processes on active planet, where crystalline minerals reveal environmental indicator of different stages of planet Earth, together with extraterrestrial rocks originated from the Moon, Asteroids and Mars. The purpose of the present study is that minerals formed at successive planet Earth with different stages are applied to be compared with different environments of the primordial Earth and extraterrestrial bodies (with global water system or not) as follows.

1. Minerals formed on the active water planet Earth have environmental information on the time and place of generation and change and the place with different structure and composition in details. Therefore, the minerals formed on active planet Earth are all different physicochemical information without any representative mineral characteristics, but shown as only simple mineral names with bulk data.

2. Minerals formed on the Earth at different reaction time of the geological units have the same mineral name, but their physicochemical information is basically different, because of different environmental conditions to be formed on Earth.

3. If we can use same mineral names both in Earth and extraterrestrial bodies, precise compositional and structural data of minerals formed on active air- and water-planet Earth are precisely different. Therefore, any minerals formed on primordial Moon and planets without detailed material-database do not suggest past existence of global water on the extraterrestrial bodies of the Solar System.

4. The present study suggests that the minerals in the Earth are considered to be solidified remnants after evaporated and fluid processes without location of atomic sites and layer molecules, which are developed further to deep interior of largere planetary bodies.

5. Author would present the data in the JpGU-AGU 2017 meeting that the remained solids by quenched processes of the carbon-bearing grains of various Earth, Asteroids and lunar rocks showing the idea and the nano-technical images by the analytical electron microscopy relatively.

6. Elements (carbon) of volatile quench solidified material (carbon inclusions) formed in the impact process are decomposed to form the surface element-resources (diamond carbon etc.) on shallow surface to deep interior on active Earth, where real origins of the internal volatile elements of the deeper mantle rocks are relatively difficult to be determined for large planetary bodies only from present location site (esp. on many developments of deeper products).

7. The present results show that carbon-bearing solidified grains by quenching are remained at all shocked events of active young Earth and primitive extraterrestrial celestial bodies widely. When we can found carbon-bearing grains in primordial satellites and planets, they are continued to keep original grains without global ocean-water system of Earth-type planets clearly as one of new results in this study of the JpGU-AGU meeting 2017.

Keywords: Earth's minerals, Quenched solids with volatiles, Various mineral characteristics

CLAY MINERALOGY OF ALTERED VOLCANIC ASH BEDS AND FACIES CORRELATION BETWEEN THE PERMIAN TO TRIASSIC BOUNDARY STRATIGRAPHIC SETS IN GUIZHOU AND SICHUAN PROVINCE OF SOUTH CHINA

*Ni na Gong¹, qian Fang

1. China University of Geosciences

Permian to Triassic is the important stage for the Earth from Paleozoic to Mesozoic, and the extinction among the Permian to Triassic is a hot topic by researchers. Many researchers had been study it by different aspect. The view of volcanism to P-T extinction was accepted to more and more researchers, and the wide distribution of Permian to Triassic nearby boundary is the important record of extinction. The mineralogy characteristic of clay mineral can provide important information of sedimentary source, and the research about it has important research significance. Successions of the Permian-Triassic boundary (PTB) altered volcanic ash beds exist in south China.

The Permian-Triassic boundary (PTB) successions in south China contain numerous altered volcanic ash beds (K-bentonites), which presents the opportunity to correlate the PTB position in both marine and non-marine PTB sections. Clay mineralogical and geochemical studies of two altered ash beds in the Chahe(CH), in Guizhou Province and Shangsi (SS) in Sichuan Province sections, in south China, deposited in littoral and interactive marine-terrestrial environments respectively, permit an investigation of the alteration of ashes and correlation of ash beds between disparate facies. The results show that the two CH altered ashes are dominated by R2 and R3 I/S clays, with 86.3 % and 84.04 % illite layers for samples SS and 57.83 % and 68.19% illite layers, respectively. The CH ash samples contain mainly kaolinite and mixed-laye illite/smectite (I/S) clays. The poorly-crystallized kaolinite is present in pseudo-hexagonal plates, and the well-crystallized kaolinite occurs in book-like aggregates in veins or cavities. Obviously, the CH ashes experienced terrestrial weathering and re-sedimentation prior to final burial and preservation, and local microenvironmental conditions control the formation of clay minerals. The SS ash samples have markedly lower $^{87}\text{Sr}/^{86}\text{Sr}$ values (0.721708 for SS-1 and 0.717225 for SS-2) than those of the CH samples (0.761077 and 0.742332). The notable difference in $^{87}\text{Sr}/^{86}\text{Sr}$ value of ash beds between the sections is attributed to variations in Rb-Sr partitioning during the chemical weathering process in different environments. The CH ash samples have notably higher $^{149}\text{Nd}/^{144}\text{Nd}$ ratios (0.512376 for CH-1 and 0.512424 for CH-2) than those of the SS samples (0.512034 for SS-1 and 0.512043 for SS-2), suggesting that the CH ashes are likely derived from continental crust and the SS ashes originate from new continental island arcs, in agreement with the REE distributions and the Ti vs. Zr, TiO_2 vs. Al_2O_3 , and Zr/ TiO_2 vs. Nb/Y discrimination plots. The occurrence of different volcanisms in PTB stratigraphic sets previously believed to be synchronous, south China, suggests that correlation between disparate facies by an ash marker is unwise without geochemical fingerprinting of the materials.

Keywords: Altered volcanic ash, illite-smectite, Sr isotopic composition, Nd isotopic composition, weathering

Understanding the origin of polycrystalline diamond, carbonado through analysis of nano-inclusions

*Hiroaki Ohfuji¹, Natsuko Asano¹, Hiroyuki Kagi²

1. Geodynamics Research Center, Ehime University, 2. Graduate School of Science, University of Tokyo

Carbonado is a type of polycrystalline diamond, which shows a grayish to black color and a massive and irregular morphology with a porous internal texture. It is distinct from ordinary mantle-derived diamonds in the following respects: extremely low carbon isotope composition (-25~-30 ‰), absence of mantle-derived primary inclusions, high concentration of radiogenic noble gases, etc. Therefore, the origin of carbonado has long been controversial. A recent study (Ishibashi et al., 2010) found several lines of evidence that H₂O-rich fluid is present within constituent diamond grains of carbonado, suggesting its formation in close association with C-H-O fluid in the Earth's mantle. However, the detail of the formation process and condition of carbonado is still unclear.

Here, we found, for the first time, primary mineral inclusions (majoritic garnets, phengite, rutile, apatite, etc.) in nano-sized negative crystals within diamond grains by detailed FE-SEM and TEM observations. Those precipitates usually occur as an assemblage of a few to several mineral phases that are mostly in euhedral forms in the negative crystals. They are most likely quenched products from silicic fluid that were trapped during the crystal growth of diamonds that comprise carbonado. The presence of these mineral phases in negative crystals suggests that the formation of carbonado occurred in fluid-saturated environments to which crustal materials (e.g. basalt) are supplied potentially by the subduction of oceanic plates or extensive collision of continental plates to form a thick mantle keel.

Keywords: Diamond, Carbonado, inclusion

CaO₈ and MgO₈ clustering in Grs₅₀Prp₅₀ garnet in diamond-bearing dolomite marble from the Kokchetav Massif

*Tomohiro Takebayashi¹, Takeaki Saito², Kunihiko Sakamaki¹, Hiroshi Suzuki^{2,1}, Yoshihide Ogasawara^{2,1}

1. Department of Earth Sciences, Resources and Environmental Engineering, Graduate school of Creative Science and Engineering, Waseda University, 2. Department of Earth Sciences, Waseda University

Grossular-pyrope garnet (ca. Grs₅₀Prp₅₀) has long been attracted about crystal chemistry, mixing properties, and P-T stabilities. Many experimental and thermodynamic studies on grossular-pyrope garnet have been conducted (e.g., Ganguly et al., 1996; Geiger, 2013; Du et al., 2016). Garnet having near the Grs₅₀Prp₅₀ composition is extremely rare in nature. Only two occurrences have been reported, so far; (1) xenocrysts in the kimberlite from Garnet Ridge, Arizona (Wang et al., 2000) and (2) diamond-bearing dolomite marble from the Kokchetav UHP Massif, Kazakhstan (e.g., Ogasawara et al., 2000; Sobolev et al., 2001). This strange garnet from the Kokchetav Massif is a main constituent silicate mineral of dolomite marble (P > 6 GPa, T = ca. 1000 °C) and is a main host mineral of abundant microdiamond (Ogasawara et al., 2000; 2005). This garnet is chemically homogeneous and has its composition range: Grs: 43-46, Prp: 39-42, and Alm: 10-16 mol%. The closest composition to Grs₅₀Prp₅₀ is Grs₄₄Prp₄₂Alm₁₀. No exsolution and no symplectite were observed.

We conducted laser Raman spectrometry on this Grs₅₀Prp₅₀ garnet in the Kokchetav UHP dolomite marble. Among the obtained Raman bands at 366, 556, and 903 cm⁻¹, we focused on the band at 366 cm⁻¹ that was assigned to R(SiO₄)⁴⁻. FWHM of this band was significantly large (24.5 cm⁻¹), compared to those of Prp (14.3 cm⁻¹ at 365 cm⁻¹) and Grs (14.0 cm⁻¹ at 372 cm⁻¹). Such a large FWHM of Grs₅₀Prp₅₀ garnet suggested that two kinds of R(SiO₄)⁴⁻ bands corresponding to Grs and Prp were obtained as one overlapped broad band because the peak positions of both bands are very close. The synthesized band from Grs and Prp end-member was well fitted to the observed band.

In the crystal structure of garnet, a SiO₄ tetrahedron is surrounded by six dodecahedra XO₈ (Geiger, 2013). A SiO₄ tetrahedron of grossular surrounded by six CaO₈, and that of pyrope by six MgO₈. The observed overlapping of two R(SiO₄)⁴⁻ bands corresponding to Grs and Prp indicates two modes for R(SiO₄)⁴⁻ in a single Grs₅₀Prp₅₀ crystal; R(SiO₄)⁴⁻ of SiO₄ surrounded by six CaO₈ (CaO₈ clustering around SiO₄) and that by six MgO₈ (MgO₈ clustering around SiO₄). Such clustering stabilized garnet of ca. Grs₅₀Prp₅₀, and could be controlled by two factors: (1) bulk chemistry near Ca:Mg = 1:1 and (2) UHP conditions. No exsolution lamella and no symplectite mean that Grs₅₀Prp₅₀ garnet was stable under low P and T once it formed at high P and T.

Reference

- Du, W., Clark, S.M., Walker, D., 2016, *American Mineralogist*, **101**, 193-204.
 Ganguly, J., Cheng, W., Tirone, M., 1996, *Contributions to Mineralogy and Petrology*, **126**, 137-151.
 Geiger, C.A., 2013, *Elements*, **9**, 447-452.
 Ogasawara, Y., 2005, *Elements*, **1**, 91-96.
 Ogasawara, Y., Ohta, M., Fukasawa, K., Katayama, I., Maruyama, S., 2000, *Island Arc*, **9**, 400-416.
 Sobolev, N.V., Schertl, H.-P., Burchard, M., Shatsky, V.S., 2001, *Doklady Earth Science*, **380**, 791-794.
 Suzuki, H., Takebayashi, T., Saito, T., Sakamaki, K., Ogasawara, Y., 2017, *JpGU Meeting abstract*.
 Wang, L., Essene, E.J., Zhang, Y., 2000, *American Mineralogist*, **85**, 41-46.

Keywords: Grossular-Pyropite Garnet, Ultrahigh-pressure, diamond, Laser Raman spectroscopy, clustering, Kokchetav

A new insight on the chloritization mechanism of biotite in hydrothermally altered granite

*Takahiro Ishii¹, Toshihiro Kogure¹, Ryosuke Kikuchi¹, Ritsuro Miyawaki², Takashi Yuguchi³

1. University of Tokyo, 2. National Museum of Nature and Science, 3. Yamagata University

Chlorite commonly forms by hydrothermal alteration of biotite in granitic rocks. This “chloritization” mechanism of biotite has been paid attention and investigated for a long time to understand alteration history of granitic rock which is one of the most common lithofacies. However, it looks that previous studies have focused either crystallographic [1, 2] or chemical aspect [3] of the chloritization, not both. This study investigated the chloritization process of biotite, by analysing both the crystal structures and chemical compositions of the chlorite. As a result, a new insight for the chloritization, simultaneous occurrence of the two transformation mechanisms, is proposed.

The rock investigated was Toki granite, distributed in Central Japan. The sample was collected from the borehole in the Mizunami Underground Research Laboratory; in the altitude range from -274m to -314 m above sea level [3]. Observation of the petrographic thin sections revealed that the granite contains biotite with various stages of chloritization. Generally, biotite grains of various chloritization are homogeneously distributed in a thin section. X-ray diffraction (XRD) patterns obtained using a Gandolfi camera confirmed that the dominant polytype of unaltered biotite is 1*M* and the polytypic group of the emerald-like coloured chlorite grains is 11*bb*. Electron microprobe analysis revealed that emerald-like coloured, completely chloritized grains contain no titanium (Ti) which is a constituent element of biotite in granite (“Ti-free chlorite”). On the other hand, element mapping of partially chloritized biotite grains indicated that the grains contain thin regions with no potassium (namely no biotite component) but with a certain amount of Ti. Considering existence of other elements, these thin regions are also considered to be chlorite (“Ti-bearing chlorite”). Quantitative analysis of these Ti-free and Ti-bearing chlorite showed different Al contents and Mg/Fe ratios between them, beside the amount of Ti. Investigation using TEM confirmed that both Ti-free and Ti-bearing chlorites are really “chlorite” , from electron diffraction and high-resolution imaging.

This compositional difference can be ascribed to different chloritization mechanisms; Ti-bearing chlorite took over the 2:1 layer from biotite, and Ti-free chlorite was formed via dissolution-recrystallization process. In biotite, Ti is expected to locate in the octahedral sheet of the 2:1 layer. Hence, chlorite transformed from biotite must contain Ti, if the 2:1 layer was inherited from biotite without significant cation diffusion. On the contrary, chlorite can be Ti-free, if the 2:1 layer was once dissolved and new 2:1 layers formed from the hydrothermal fluid. In this case, Ti formed titanite, CaTiSiO_5 , which is common within chloritized grains, with calcium and silicon transported via the fluid. In TEM, Ti-bearing chlorite showed a diffraction pattern indicating a mixture of different polytypic groups, indicating structural discontinuity with completely chloritized grains which were 11*bb* from XRD. 11*bb* is considered to be the most stable polytypic group and expected to form if chlorite was formed from solution. However, if chlorite was transformed from biotite via a solid-to-solid pathway inheriting the 2:1 layer, complete 11*bb* stacking may not be expected owing to the difference of the interlayer structures between biotite and chlorite [2]. Finally, high-resolution imaging support that Ti-bearing chlorite inherited the 2:1 layer from biotite, because this chlorite has 2:1 layers whose orientation is uniform, which is the same characteristic as biotite-1*M*. On the other hand, Ti-free chlorite consists of 2:1 layers whose orientation is considerably disordered.

[1] Veblen DR., Ferry JM. (1983). A TEM study of the biotite-chlorite reaction and comparison with

petrologic observations. *American Mineralogist*, 68, 1160-1168.

[2] Kogure T., Banfield JF. (2000). New insights into the mechanism for chloritization of biotite using polytype analysis. *American Mineralogist*, 85, 1202-1208.

[3] Yuguchi T., Sasao, E., Ishibashi M., Nishiyama, T. (2015). Hydrothermal chloritization process from biotite in the Toki granite, Central Japan: Temporal variations of the compositions of hydrothermal fluids associated with chloritization. *American Mineralogist*, 100, 1134-1152.

Keywords: chloritization, biotite, hydrothermal alteration, granite

Grs₅₀Prp₅₀ garnet-bearing composite inclusion in Cr-rich pyrope from Garnet Ridge, the Colorado Plateau

*Hiroshi Suzuki^{1,2}, Tomohiro Takebayashi², Takeaki Saito¹, Kunihiro Sakamaki², Yoshihide Ogasawara^{1,2}

1. Department of Earth Sciences, Waseda University, 2. Department of Earth Sciences, Resources and Environmental Engineering, Graduate school of Creative Science and Engineering, Waseda University

Garnet having near Grs₅₀Prp₅₀ composition is very rare in nature because of the large difference in ionic radii between Ca²⁺ and Mg²⁺. So far, only two occurrences have been reported from Garnet ridge, Arizona (Wang *et al.*, 2000) and the Kokchetav UHP Massif, Kazakhstan (e.g., Ogasawara *et al.*, 2000; Sobolev *et al.*, 2001). At Garnet Ridge, Wang *et al.* (2000) described four grains of Grs₅₀Prp₅₀ garnet as a constituent of composite inclusions in pyrope-rich garnet in kimberlitic diatremes. In the Kokchetav UHP Massif, Grs₅₀Prp₅₀ garnet is a major constituent mineral of UHP dolomite marble, and contains abundant microdiamonds. Takebayashi *et al.* (2017) has stated that CaO₈ and MgO₈ clustering around a SiO₄ tetrahedron stabilized ca. Grs₅₀Prp₅₀ compositions on the basis of the overlapping of R(SiO₄)⁴⁻ Raman bands corresponding to Grs (372 cm⁻¹) and Prp (364 cm⁻¹), and considered that two main factors controlled the formation of this strange garnet; (1) the bulk chemistry of the host rock (Ca:Mg = 1:1) and (2) UHP conditions.

Recently, we discovered one grain of Grs₅₀Prp₅₀ garnet from the Garnet Ridge; the garnet occurs as a constituent of composite inclusion in the host Cr-rich pyrope (Group A by Sakamaki *et al.*, 2016), which is of garnet Iherzolite origin. Cr-rich pyrope (Group A) is an original material for Cr-poor pyrope (Group B) during mantle metasomatism. The found composite inclusion, which shows spherical form measuring 150 μm across, consists of pargasite and dolomite with minor Cr-spinel, phlogopite and apatite. The other composite inclusions consist of pargasite, dolomite, Cr-spinel with minor apatite and magnesite. We conducted laser Raman spectrometry on this Grs₅₀Prp₅₀ garnet, and focused on the band attributed to R(SiO₄)⁴⁻ at 365 cm⁻¹. The overlapping of R(SiO₄)⁴⁻ bands corresponding to Grs and Prp in a single Grs₅₀Prp₅₀ crystal was observed. Our results of Raman spectrometry were consistent with those of the Kokchetav Grs₅₀Prp₅₀ garnet by Takebayashi *et al.* (2017).

Almost all composite inclusions contain dolomite/magnesite and show rounded or spherical form. This suggests that these composite inclusions were trapped carbonate-silicate melt during the mantle metasomatism. The Grs₅₀Prp₅₀ garnet in the found composite inclusion was formed from such trapped melt which had the bulk chemistry, near Ca:Mg = 1:1, at very high pressure.

The Grs₅₀Prp₅₀ garnet described by Wang *et al.* (2000) could have formed by the same process from trapped carbonate-silicate melt, and the inclusion Grs₅₀Prp₅₀ garnet was not in equilibrium with the host pyrope-rich garnet. Their interpretation about the genesis of Grs₅₀Prp₅₀ garnet including very low formation temperature based on the coexistence with the host may be wrong.

References

- Ogasawara, Y., Ohta, M., Fukasawa, K., Katayama, I., Maruyama, S., 2000, *Island Arc*, **9**, 400-416.
- Ogasawara, Y., Sakamaki, K., Takebayashi, T., Suzuki, H., Saito, T., 2016, *AGU Fall Meeting*, SR33A-2673.
- Sakamaki, K., Sato, Y., Ogasawara, Y., 2016, *Progress in Earth and Planetary Science*, **3**, 1-17.
- Sobolev, N.V., Schertl, H.-P., Burchard, M., Shatsky, V.S., 2001, *Doklady Earth Science*, **380**, 791-794.
- Takebayashi, T., Saito, T., Suzuki, H., Sakamaki, K., Ogasawara, Y., 2017. *JpGU Meeting Abstract*.
- Wang, L., Essene, E.J., Zhang, Y., 2000, *American Mineralogist*, **85**, 41-46.

Keywords: Grossular-pyrope garnet, Garnet Ridge, Kimberlite, Laser Raman spectroscopy, Colorado Plateau, Cr-rich pyrope